Marine Geology 271 (2010) 93–105

Contents lists available at ScienceDirect

Marine Geology

journal homepage: www.elsevier.com/locate/margeo

Multi-proxy records of environmental changes in Hudson Bay and Strait since the final outburst flood of Lake Agassiz–Ojibway

Torsten Haberzettl [a,b,d,*], Guillaume St-Onge [a,b], Patrick Lajeunesse [c]

[a] Institut des sciences de la mer de Rimouski (ISMER), Université du Québec à Rimouski, 310, allée des Ursulines, Rimouski, Québec, Canada G5L 3A1
[b] GEOTOP Research Center, P.O. Box 8888, Succ. Centre-ville, Montréal, Québec, Canada H3C 3P8
[c] Centre d'études nordiques and Département de Géographie, Université Laval, Québec, Québec, Canada G1V 0A6
[d] Physical Geography, Institute of Geography, Friedrich-Schiller-University Jena, Löbdergraben 32, 07743 Jena, Germany

ARTICLE INFO

Article history:
Received 15 April 2009
Received in revised form 20 November 2009
Accepted 23 January 2010
Available online 10 February 2010

Keywords:
postglacial sedimentation
marine sediment cores
paleoenvironmental reconstruction
Hudson Bay
Hudson Strait

ABSTRACT

In this study postglacial continuous high-resolution data from five marine sediment cores from Hudson Bay and Hudson Strait are presented. Up to now studies in this area focused on the distinction between large scale climatic variations like the glacial–postglacial transition or most recent processes. However, as demonstrated in this study, using sedimentological, geochemical and geophysical parameters, postglacial sediments provide provenance signals distinguishing between Proterozoic Dubawnt Group sediments, Paleozoic limestone sources underlying parts of Hudson Bay and Strait and Precambrian granitoids from the Canadian Shield. For example it is shown that redistribution of Dubawnt Group sediments is of minor importance after the outburst flood of Lake Agassiz. Paleoproductivity indicators also give insights into paleotemperature trends. These are in phase with terrestrial reconstructions from that area. Colder conditions in Hudson Strait until ca. 4500 cal BP followed by a signal of warmth until ca. 4000 cal BP are suggested. Subsequently, a cool interval lasting until approximately 2000 cal BP occurred. Thereafter, a gradual decrease in temperature was observed reaching lowest values during the Little Ice Age period and increasing again afterwards.

1. Introduction

High latitude regions of eastern North America have experienced large environmental variations during the Late Quaternary (Henderson, 1990; Josenhans and Zevenhuizen, 1990; Kerwin et al., 2004; Laymon, 1992; Overpeck et al., 1997; Sawada et al., 1999). During the last two decades much effort has been put in the reconstruction of paleoenvironmental conditions of the sub-Arctic Hudson Bay marine system, consisting of Foxe Bay, Hudson Bay and Hudson Strait (Hare et al., 2008). However, these investigations mainly focused on glacial geomorphology (Josenhans and Zevenhuizen, 1990; Lajeunesse, 2008; Lajeunesse and Allard, 2003a; Lajeunesse and Allard, 2003b) or seismostratigraphy (Hill et al., 1999; Lavoie et al., 2008) in combination with sediment cores that allowed to identify large scale variations of environmental change such as the deglacial to postglacial transition (Bilodeau et al., 1990; Gonthier et al., 1993; Hall et al., 2001; Hardy, 2001; Jennings et al., 2001). Alternatively, continuous or high-resolution studies focused on the last outburst flood of Lake Agassiz around 8.5 ka causing a prominent red bed (red layer), consisting of probably reworked sediments originating from the Dubawnt Group (Hall et al., 2001; Kerwin, 1996) in the spillway (Lajeunesse and St-Onge, 2008; St-Onge and Lajeunesse, 2007) and its consequences with respect to the global climate (Alley and Ágústsdóttir, 2005; von Grafenstein et al., 1998). Latest studies focus on modern and most recent processes affecting sediments of Hudson Bay (Hare et al., 2008; Kuzyk et al., 2008). Only one study has considered the Holocene potential of Hudson Bay sediments for paleoenvironmental reconstructions looking at fluviodeltaic deposits of rivers discharging into Hudson Bay (Jenner and Piper, 2002). Nevertheless, sediments of Hudson Bay and Strait hold the complete postglacial history of that area provided that the "right" coring location is chosen. The main problem in Hudson Bay is the scarcity of postglacial sediments. Throughout the entire area postglacial deposition is minimal and sediment seems only to accumulate in very deep parts and pockets which are not affected by redistribution caused by currents (Henderson, 1990). Intensively studied areas along the southern coast have revealed that ice scouring and wave action disturb or even remove surficial Holocene sediments (Hare et al., 2008). On the regional scale sediment distribution is hence primarily related to bathymetry and, secondarily to the proximity of the coastline, especially offshore major rivers (Henderson, 1990). It was estimated that the area of postglacial sedimentation is only approximately 82,600 km^2, which corresponds to 10% of the total surface area of Hudson Bay (Hare et al., 2008).

Here we present continuous and high-resolution sediment records from the central Hudson Bay area, the east coast of Hudson Bay and western Hudson Strait (Fig. 1), enabling a deeper insight into the

* Corresponding author. Physical Geography, Institute of Geography, Friedrich-Schiller-University Jena, Löbdergraben 32, 07743 Jena, Germany. Tel.: +49 3641 9 48815; fax: +49 3641 9 48812.
E-mail address: Torsten.Haberzettl@uni-jena.de (T. Haberzettl).

0025-3227/$ – see front matter © 2010 Elsevier B.V. All rights reserved.
doi:10.1016/j.margeo.2010.01.014

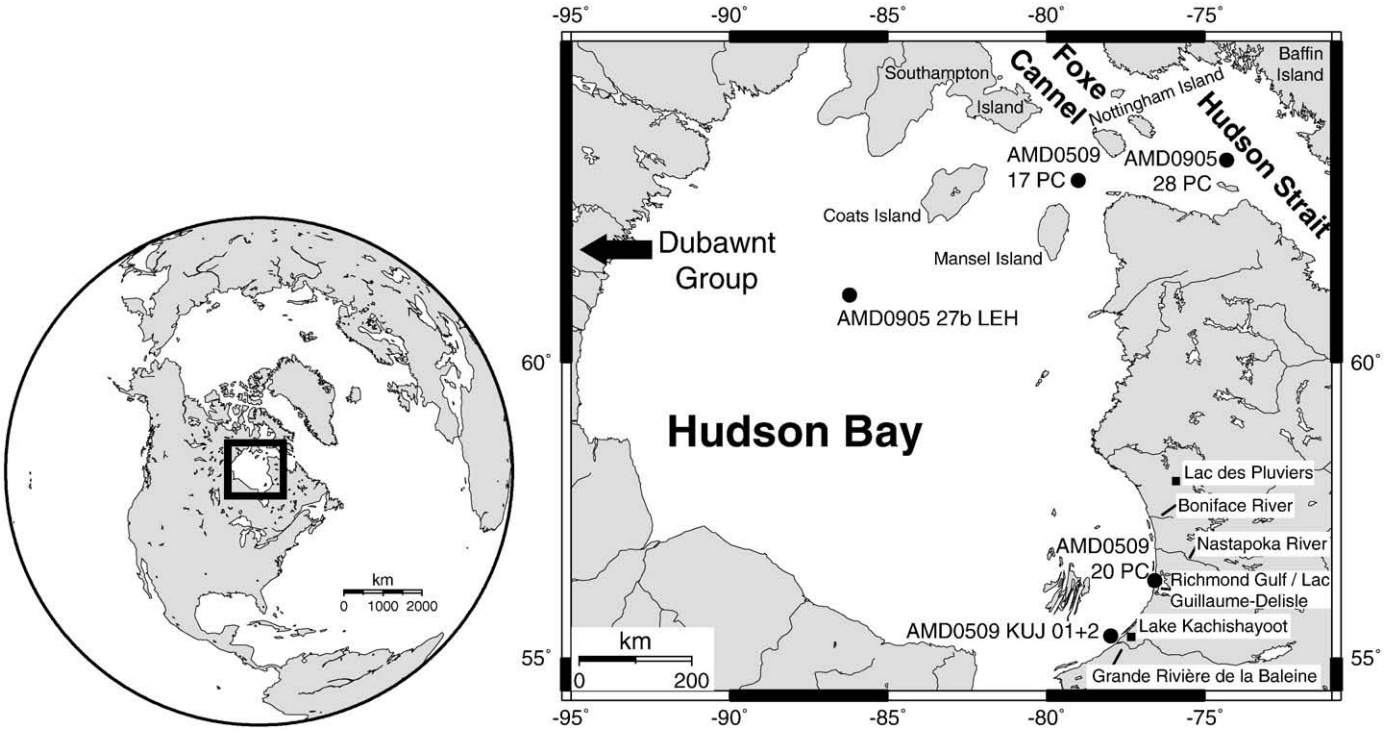

Fig. 1. Map of the research area showing the Hudson Bay marine system consisting of Hudson Bay, Hudson Strait and the Foxe Basin. Also illustrated are the sampling sites of the sediment cores used for this study (black dots), as well as the locations mentioned in the text. The basic map was created using OMC (Weinelt, 1996–2004).

development of postglacial paleoenvironmental and provenance changes of an area which was demonstrated to be very susceptible to climate change (Henderson, 1990; Kerwin et al., 2004; Overpeck et al., 1997).

2. Regional setting and Late Quaternary regional stratigraphy

With a total surface area of 1.24×10^6 km^2 the sub-Arctic Hudson Bay marine system (Fig. 1) is the largest inland sea in the world exhibiting a general counter-clockwise circulation (Hare et al., 2008; Prinsenberg, 1986). North Atlantic water does not penetrate Hudson Bay. It re-circulates in Hudson Strait where it mixes with outflowing Hudson Bay and Foxe Basin water before leaving along the southern Hudson Strait again (Hare et al., 2008). Being one of the most southerly extensions of Arctic marine waters Hudson Bay experiences an annual sea-ice cover and receives ~30% of the total Canadian runoff by river discharge (Kuzyk et al., 2008). On the background of glacio-isostatic uplift, postglacial sediments may also result to a large extent from the erosion and remobilization of glacigenic deposits and the effects of sea-ice rafting. In contrast, aeolian input is believed to be of minor importance (Henderson, 1990). Riverine sediment input is estimated to be in the order of $10.2^{+1.2}/_{-2}$ Mt yr^{-1}, atmospheric input 0.74 ± 0.3 Mt yr^{-1}, coastal erosion $18^{+9.5}/_{-0}$ Mt yr^{-1}, and resuspension 120 Mt yr^{-1} (Hare et al., 2008).

During the Late Wisconsinan glaciation the Hudson Bay marine system was covered by the Laurentide Ice Sheet (Dyke and Prest, 1987). The weight of the ice caused displacement of the mantle and depression of the land surface to elevations at least 100 to 315 m below the present surface (Hillaire-Marcel, 1976; Shilts, 1986). Hudson Strait was the world's largest glacial outlet, draining approximately one-third to one-quarter of the ice sheet directly into the North Atlantic (Kerwin, 1996). Deglaciation of North America resulted in the development of the ice-dammed proglacial Lake Agassiz–Ojibway along the southern margin of the Laurentide Ice Sheet (Lajeunesse and St-Onge, 2008). The rapid collapse of this ice sheet culminated in the catastrophic northward drainage of this lake into the North Atlantic around 8500 cal BP (Barber et al., 1999; Lajeunesse and St-Onge, 2008). Following deglaciation and the lake drainage, the glacio-isostatically depressed basin of Hudson Bay was invaded by the Tyrrell Sea waters (Hillaire-Marcel, 1976; Lajeunesse, 2008). Since that time, the rate of land emergence fell from about 10 m per century at 8000 BP (Allard and Seguin, 1985; Lajeunesse and Allard, 2003a) to about 1 m per century at ~2800 BP (Allard and Tremblay, 1983). Emergence rate today reaches 1.3 cm yr^{-1} (Bégin et al., 1993).

Depending on the location, seismic studies reveal three or more seismo-stratigraphic units overlying the acoustic basement (Bilodeau et al., 1990; Gonthier et al., 1993; Hardy, 2001; Josenhans et al., 1988; Lavoie et al., 2008): 1. acoustically massive subaqueous ice-contact and draped glaciomarine deposits associated with the retreat of the Quebec–Labrador Ice Sector of the Laurentide Ice Sheet; 2. acoustically strongly stratified paraglacial deposits; and 3. acoustically poorly stratified postglacial deposits. Sediment cores from the top of this seismo-stratigraphic unit through the uppermost deposits show three to four lithostratigraphical units (Bilodeau et al., 1990): the lowest is a grey diamicton consisting of gravels in a clay matrix deposited in a glaciomarine environment, probably in an ice-contact or ice-proximal setting. The second unit consists of alternating rythmites and clayey mud lenses. The uppermost sediments consist of bioturbated brownish grey clayey mud (Bilodeau et al., 1990) in some locations overlaid by distal fluviodeltaic sediments (Gonthier et al., 1993).

3. Materials and methods

3.1. Core sampling

Cores AMD0509-27bLEH, AMD0509-KUJ01PC, AMD0509-KUJ02PC, AMD0509-20PC, AMD0509-17PC and AMD0509-28PC (hereinafter referred to as cores 27, KUJ01, KUJ02, 20, 17 and 28) were collected as part of the ArcticNet program aiming for regions with high Holocene sedimentation rates using piston and gravity corers onboard the ice-breaker CCGS Amundsen in 2005 (Fig. 1). The sites were carefully selected using the 3.5 kHz sub-bottom profiler (Knudsen 320R) and multibeam echosounder (Kongsberg-Simrad EM-300) to avoid areas

Table 1
Coordinates of the retrieved cores.

Core number	Abbreviation	Latitude (°)	Longitude (°)	Water depth (m)	Core length (cm)	Region
AMD0509-27bLEH	27	61.0533	−86.2138	245	253	Cental Hudson Bay
AMD0509-KUJ01PC	KUJ01	55.3998	−77.9767	116	395	19 km off Grande-Rivière-de-la-Baleine
AMD0509-KUJ02PC	KUJ02	56.4394	−77.8530	127	330	19 km off Grande-Rivière-de-la-Baleine
AMD0509-20PC	20	56.3839	−76.5803	104	410	Nastapoka Sound
AMD0509-17PC	17	62.7574	−79.0012	395	351	Center of Hudson Bay marine system
AMD0509-28PC	28	63.05	−74.3147	430	410	Western Basin of Hudson Strait

affected by mass wasting deposits or iceberg scouring. Coring details (coordinates, water depth, length of cores, etc.) are given in Table 1.

3.2. Laboratory methods

In the laboratory, the cores were run for wet bulk density and low field volumetric whole core magnetic susceptibility (k) using a GEOTEK Multi Sensor Core Logger (MSCL). For core 27, mass susceptibility (X) was calculated by dividing k by density. The cores were then split, photographed and described. Color reflectance measurements were performed on fresh cores using a hand-held X-rite DTP22 digital swatchbook spectrophotometer. Reflectance data are reported as a^* from the widely used Commission Internationale de l'Éclairage (CIE) color space, whereas a^* ranges from +60 (red) to −60 (green).

Grain size analyses were carried out at ISMER (Institut des sciences de la mer de Rimouski) in sampling intervals ranging from 10 to 1 cm depending on the facies characteristics. Prior to grain size analyses, the samples were added to a Calgon electrolytic solution (sodium hexametaphosphate) and rotated for about 3 hours using an in-house rotator. The samples were then sieved (2 mm) and disaggregated in an ultrasonic bath for 90 s prior to their analysis. Disaggregated samples were then analyzed with a Beckman-Coulter LS-13320 (0.04 to 2000 µm) laser sizer. The results of at least three runs were averaged. Generally, mean values are used for interpretation. For core 27, the fraction 10–100 µm was summed up separately.

Sediment samples taken every 10 cm from cores 17, 28 and KUJ01 were dried, ground and analyzed for Total Carbon (TC) and Total Nitrogen (TN) contents using a Carlo-Erba™ elemental analyzer at the GEOTOP research center. Measurements were performed twice and averages were used for interpretation. If differences were larger than 0.1% for TC or 0.01% for TN, values were excluded from the interpretation. Total Inorganic Carbon (TIC) is based on direct coulometric measurements using a UIC™ coulometer at the GEOTOP research center. Total Organic Carbon (TOC) was determined using the difference between the TC measurements (from elemental analysis) and TIC content from coulometric measurements. C/N values represent atomic ratios of TOC to TN.

Samples for radiocarbon dating were submitted to IsoTrace, Toronto, Canada and Beta Analytics Inc., Miami, Florida, USA (Table 2). Radiocarbon ages were calibrated using the online CALIB 5.0.2 software (Stuiver et al., 2005) and the marine dataset (Hughen et al., 2004).

Uncalibrated ages from the literature used for comparison were calibrated with the same software and results are given as cal BP in brackets after the uncalibrated original dates given as BP. To account for the marine reservoir effect, the Marine Reservoir Correction Database of the software was used averaging known ΔR values and ΔR errors of surrounding localities (Barber et al., 1999; McNeely et al., 2006), with ΔR values ranging from −60 to 280 (±50) corresponding to a reservoir effect of 230 to 540 (±50) yrs depending on the coring site. Calibrated ages are given as median ages with 2σ errors. In sediment cores containing the red bed attributed to the outburst flood of Lake Agassiz-Ojibway (Lajeunesse and St-Onge, 2008; St-Onge and Lajeunesse, 2007) this was assumed to represent an age of 8470 cal BP (Barber et al., 1999).

4. Results

Cores KUJ01 and KUJ02 showed identical results in all parameters. Hence, KUJ01 being the longer of the two cores will be taken as representative for that area.

4.1. Lithologies

The red bed attributed to the outburst flood of Lake Agassiz was only recovered in core 27 from 147 cm to the base of the record and in core 28 from 296 to 304 cm. After core splitting, all cores (including cores 27 and 28 above the red bed) consisted of silty brownish sediments with many black spots, occasional shell fragments and drop stones as well as traces of bioturbation. While the cores from Hudson Strait (17 and 28, Fig. 1) are characterised by more greenish color variances (5Y 4/2 and 5Y 3/2), the cores from Hudson Bay (Fig. 1) are grey (5Y 5/1). After oxidization, the black spots disappeared. Traces of bioturbation were most intense in core 20 from Nastapoka Sound (Fig. 1). No gas cracking due to the high organic nature of the postglacial sediments as it was found in other records from that area (Hardy, 2001) was observed in the recovered cores.

Table 2
AMS radiocarbon dates. Median ages were used for the age–depth models presented in Fig. 2.

Core	Sediment depth (cm)	^{14}C age (BP)	Error	Sample description	Median cal. age (cal BP)	2σ age range (cal BP)	Lab no.
AMD0509-17PC	6	490	50	Valve of pelecypod	Modern	Modern	TO-13036
AMD0509-17PC	75	850	50	Unidentified shell fragments	415	300–500	TO-13037
AMD0509-17PC	302	2930	60	Unidentified shell fragments	2610	2400–2750	TO-13038
AMD0509-20PC	34.5	1090	50	Valve of pelecypod	540	455–635	TO-13039
AMD0509-20PC	50	1340	40	Unidentified shell fragments	730	640–850	Beta-219882
AMD0509-20PC	109.5	1820	50	Valve of pelecypod	1220	1075–1320	TO-13040
AMD0509-28PC	41	3150	40	Unidentified shell fragments	2870	2750–2990	Beta-221965
AMD0509-28PC	210	7800	40	Unidentified shell fragments	8220	8105–8330	Beta-221964
AMD0509-KUJ01PC	47	2360	40	Unidentified shell fragments	1890	1765–2015	Beta-219881

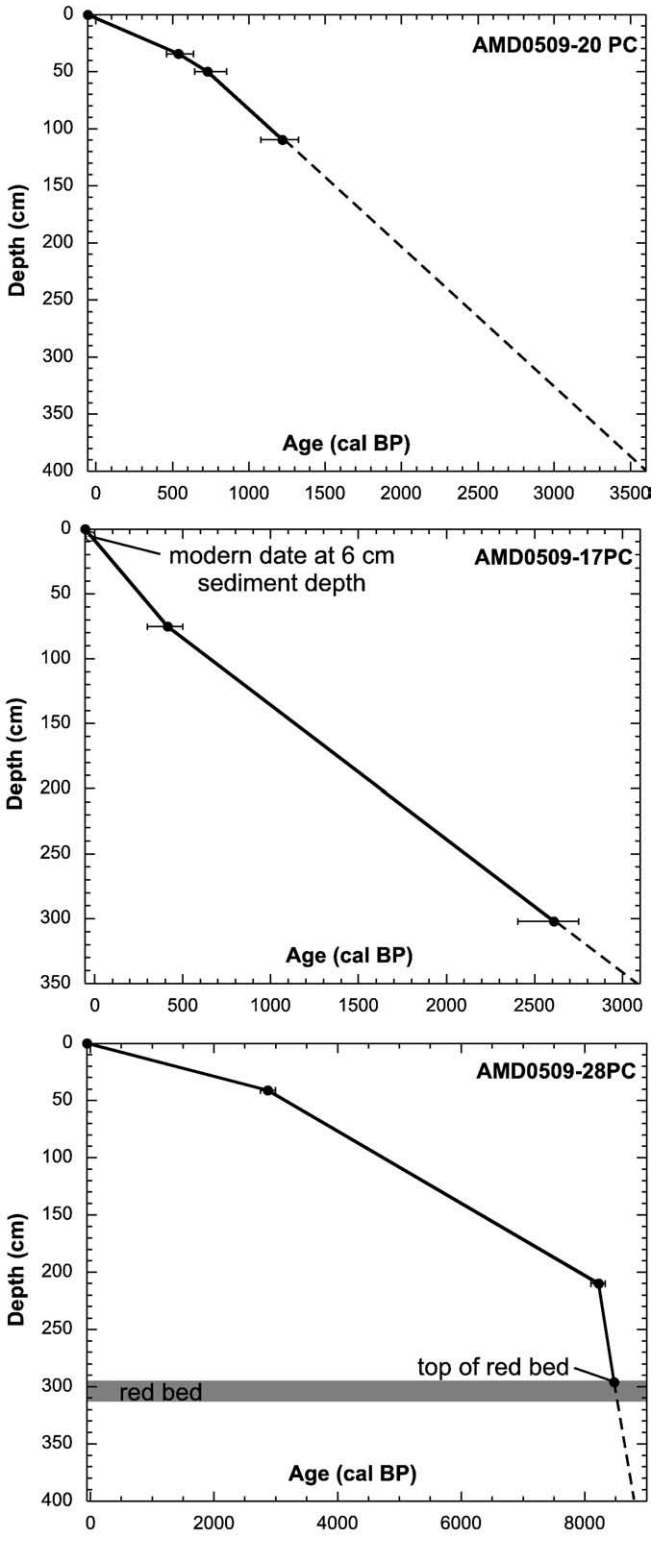

Fig. 2. Age–depth models for cores 20, 17 and 28.

4.2. Chronologies

Except for the lowermost ^{14}C age in core 28 (8220 cal BP, Fig. 2), most radiocarbon ages are younger than 3000 cal BP (Table 2), resulting in a good coverage of Late Holocene sedimentation. However, the lack of dates below 109.5 cm in core 20 only allows an approximation by linear extrapolation before $1220^{+100}/_{-145}$ cal BP (Fig. 2). The uppermost date in core 17 at 6 cm is of modern age, which confirms the age model of that core showing a slight increase in deposition above 75 cm sediment depth (after $415^{+85}/_{-115}$ cal BP). In general, the age models constructed by linear interpolation using the sediment water interface as year of coring (i.e., 2005 or −55 cal BP) show rather constant deposition. In core 28, sedimentation rates sharply decrease after deglaciation, i.e., after 8220 cal BP (Fig. 2). Mean postglacial sedimentation rates are 0.17 mm a^{-1} for core 27 (taking the red bed as the only available benchmark), 0.86 mm a^{-1} for core 20, 1.13 mm a^{-1} for core 17 and 0.26 mm a^{-1} for core 28.

There is only one date of 1890 ± 125 cal BP at 47 cm in core KUJ01 (Fig. 4). Linear interpolation between the sediment water interface and this date would result in an average sedimentation rate of 0.25 mm a^{-1} and in an age of the base of the core exceeding by far postglacial deposition. However, there is no indication of a change in lithology or even rhythmically bedded sediments as they are described in a core 10 km away from the coring location of KUJ01 (Bilodeau et al., 1990; Gonthier et al., 1993). Therefore, no age model was constructed for that core.

In the following section, results of each core are presented separately following the anticlockwise direction of the surface currents in Hudson Bay (for locations of all the cores see Fig. 1):

4.3. Core 27 (central Hudson Bay)

Core 27 is mainly characterised by high values in all measured parameters within the previously identified and described zone of the red bed (St-Onge and Lajeunesse, 2007). From the base to the top of the red bed, the most striking feature is the negative correlation of k and a^* as well as a sharp decrease in mean grain sizes from ca. 14 to 6 µm (Fig. 3). Above the red bed k, X and density show a constant decrease to very low values (k: <35 10^{-5} SI; density: <1.6 to even 1.2 g cm^{-3}) to the top of the record. After a lowering to intermediate values a^*, mean grain sizes and the 10–100 µm grain size fraction are constant above the red layer until ~100 cm. At ~100 cm there is another considerable decrease in these parameters. Above values are constant but low (mean grain sizes: ca. 3 µm, Fig. 3).

4.4. Core KUJ01 (19 km off Grande-Rivière-de-la-Baleine)

Core KUJ01 is dominated by an increase from bottom to top in all parameters except for TOC and TN (Fig. 4). This increase is characterised by a small slope in the lower and a rather steep slope in the upper part of the record. The TOC and TN profiles illustrate an opposite pattern reaching lowest values where most other parameters peak out (~25 cm). Variation in grain sizes and also absolute values for the mean are rather low (range: 2.6–4.1 µm). Molar C/N ratios vary from 8.3 to maximum values of up to 11.5.

4.5. Core 20 (Nastapoka Sound)

The most characteristic element of core 20 is a prominent shift visible in a^*, k and density at 260 cm (Fig. 5). Below a^* and k values are on a rather low level whereas above values increase with enhanced variability. The opposite is the case for density showing lower values above 260 cm. Additionally, k and density have a pronounced maximum at 350 cm and a minimum at 85 cm (Fig. 5). Grain size variations are in a very narrow range with means only varying from 3 to 5.5 µm and a slight decreasing trend from the bottom to the top of the record.

4.6. Core 17 (center of Hudson Bay marine system)

Negative a^* values, C/N and density reveal little variations in core 17 (Fig. 6). Density ranges around 1.6 g cm^{-3} with two small outliers at 220 and 125 cm, respectively. Only to the top of the core

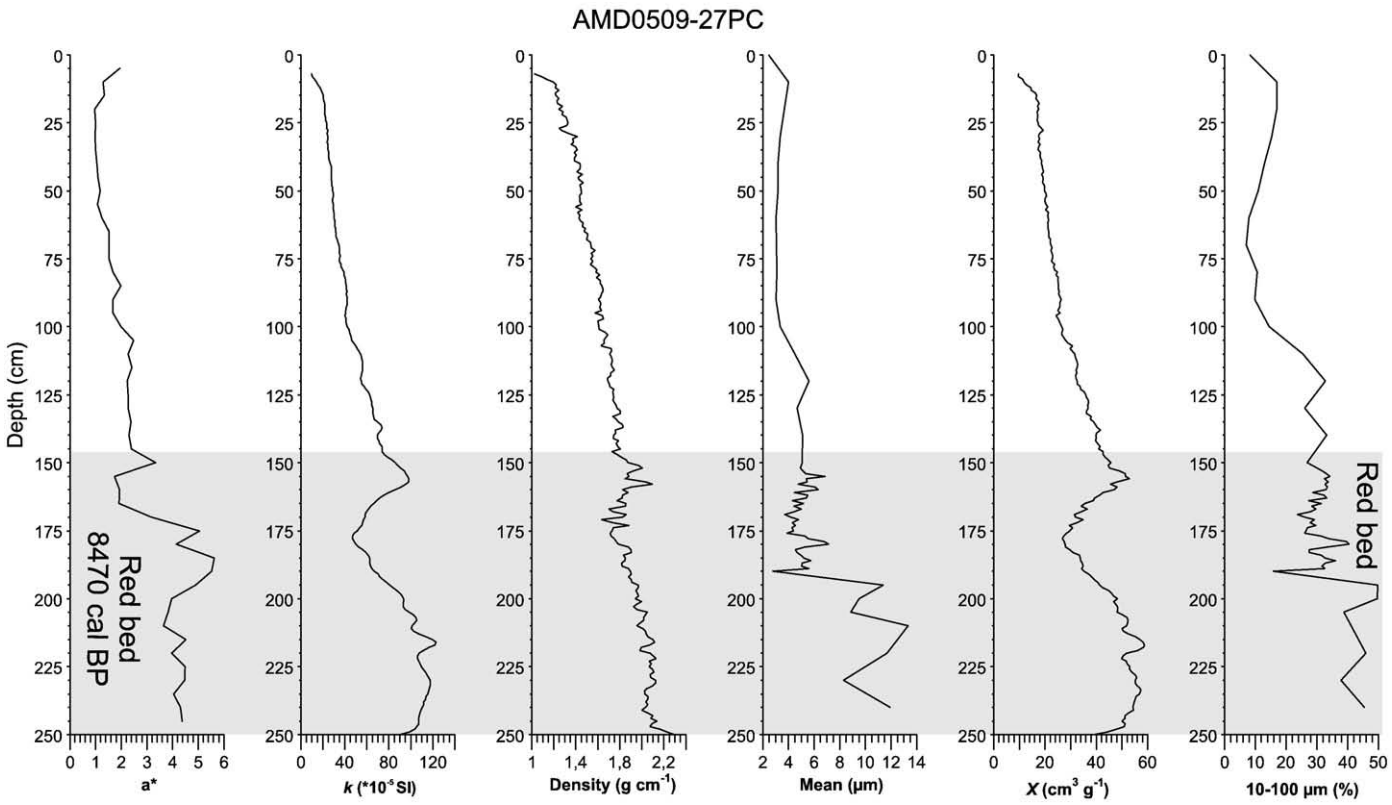

Fig. 3. Sedimentological, geochemical and physical properties of core 27.

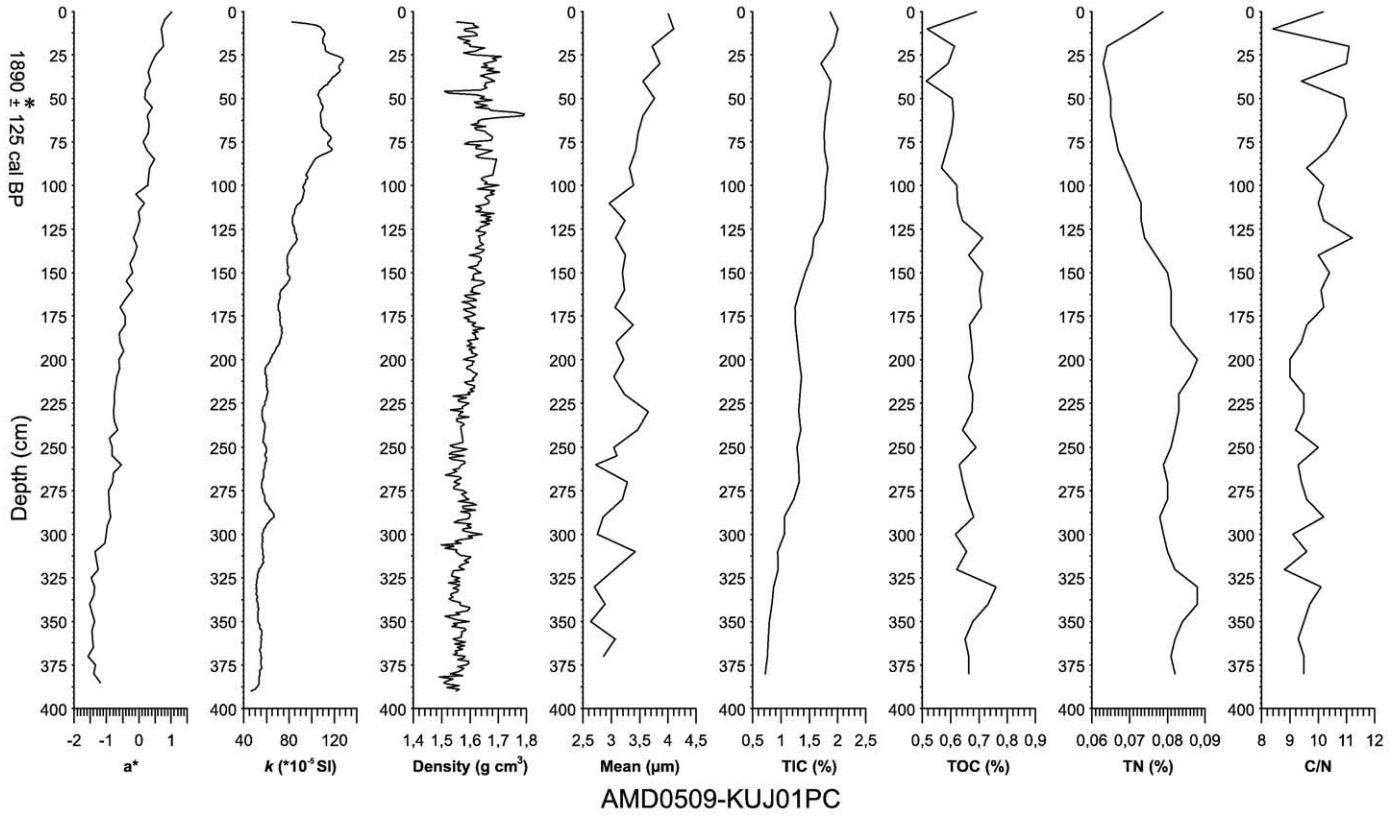

Fig. 4. Sedimentological, geochemical and physical properties of KUJ01. Additionally, the only available radiocarbon date in KUJ01 is shown.

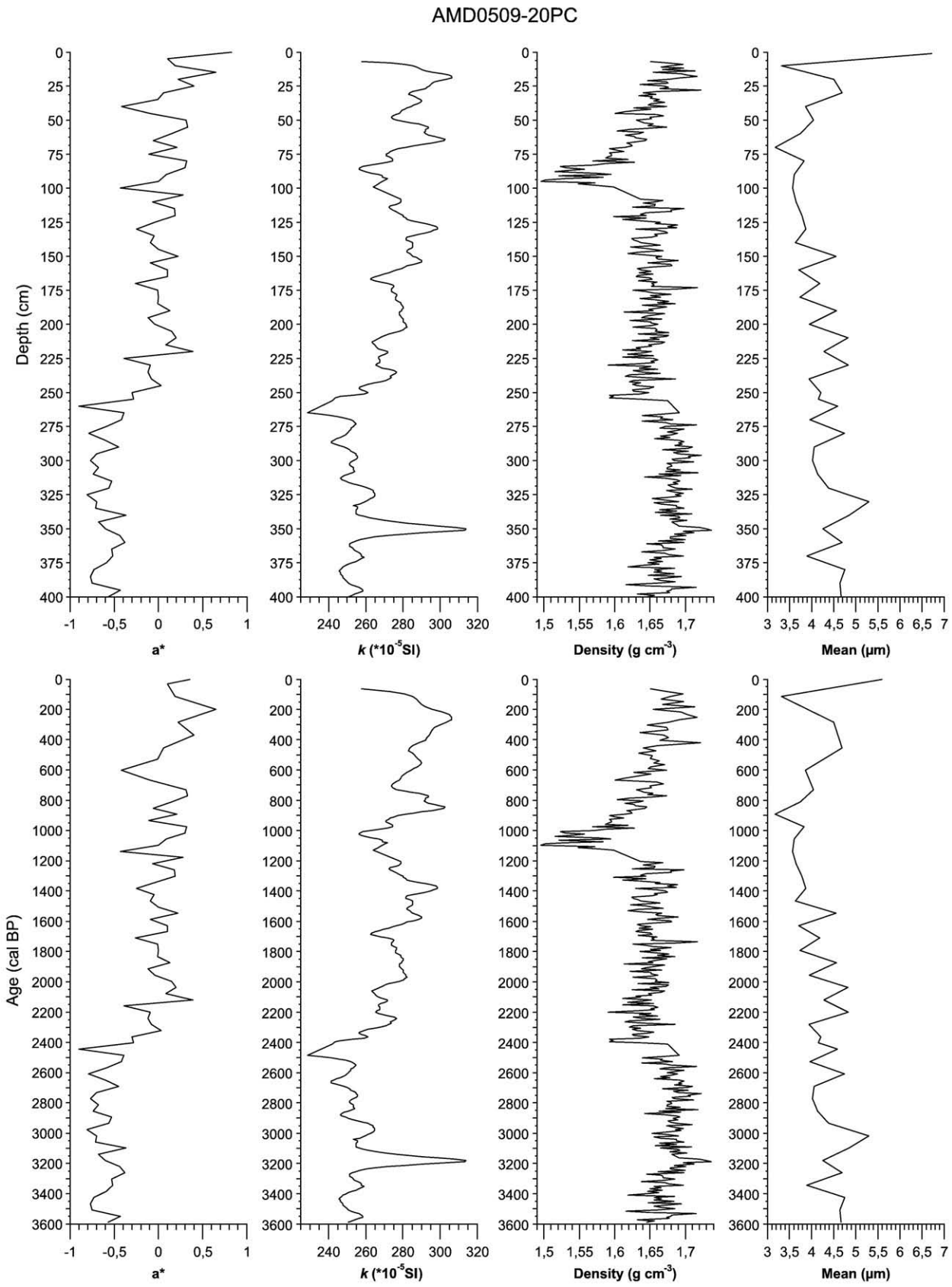

Fig. 5. Sedimentological, geochemical and physical properties of core 20 plotted on a depth scale (top), as well as on an age scale (bottom).

values decrease slightly (Fig. 6). *C/N* ratios oscillate around 10 (average: 9.77). *k* shows the lowest values in that record (8–45 10^{-5} SI). However, together with grain sizes and TIC, it rises contemporaneously from the bottom of the record to the top with a marked shift to higher values starting at ~150 cm. Showing an opposite pattern (TIC vs. TN: $r = -0.7$) TOC and TN values decrease constantly from the

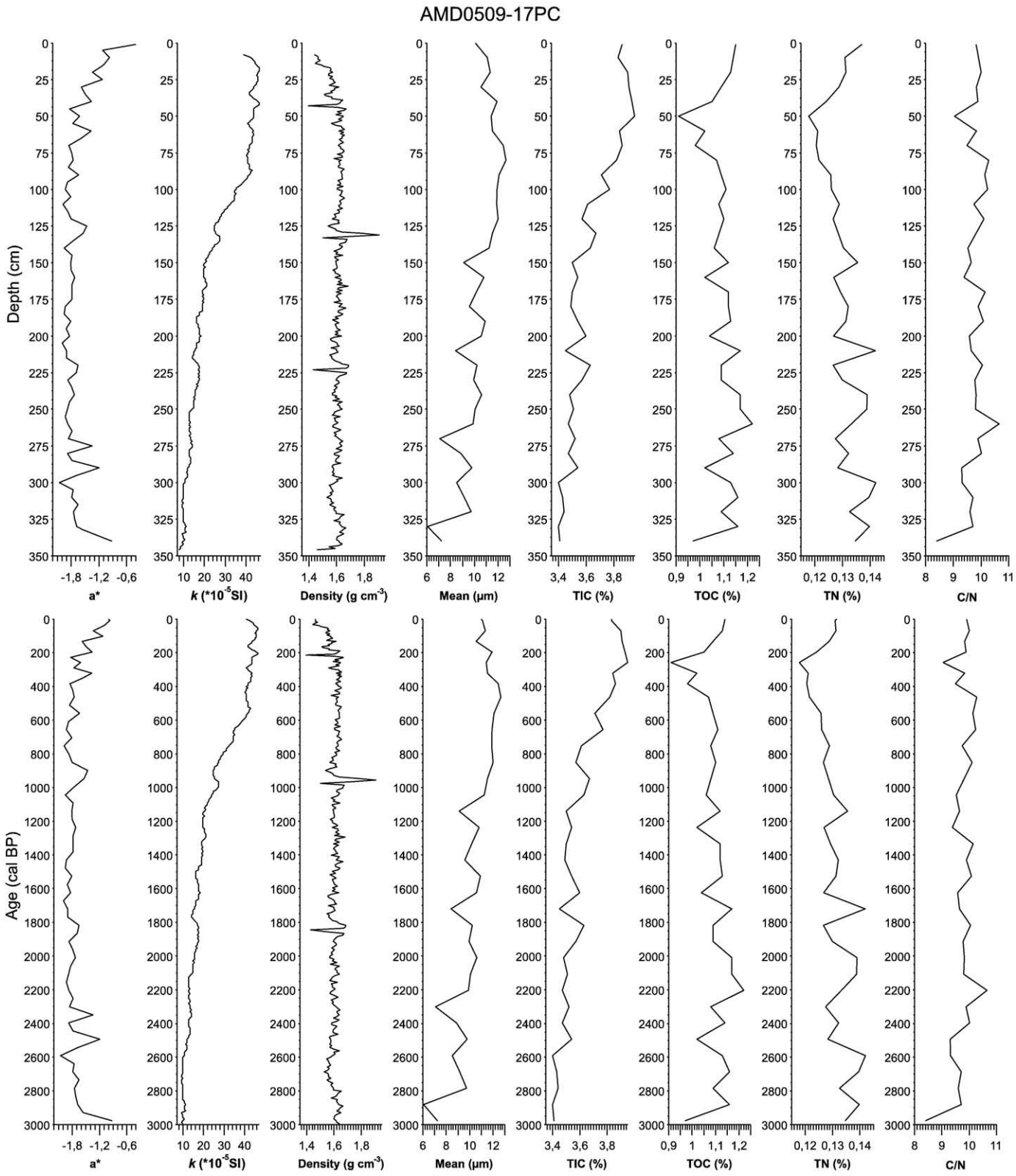

Fig. 6. Sedimentological, geochemical and physical properties of core 17 plotted on a depth scale (top), as well as on an age scale (bottom).

bottom of the record to 50 cm, where the lowest value of the record is reached. Although, values around 50 cm are lowest in this record they are higher than in the other cores. Above 50 cm, TOC and TN values rise again to values observed at the bottom of the record (Fig. 6).

4.7. Core 28 (Western Basin of Hudson Strait)

The most characteristic feature of core 28 is the occurrence of the red bed between 296 and 304 cm sediment depth yielding highest values of a^* of the record (Fig. 7). After reaching a value of 6, values

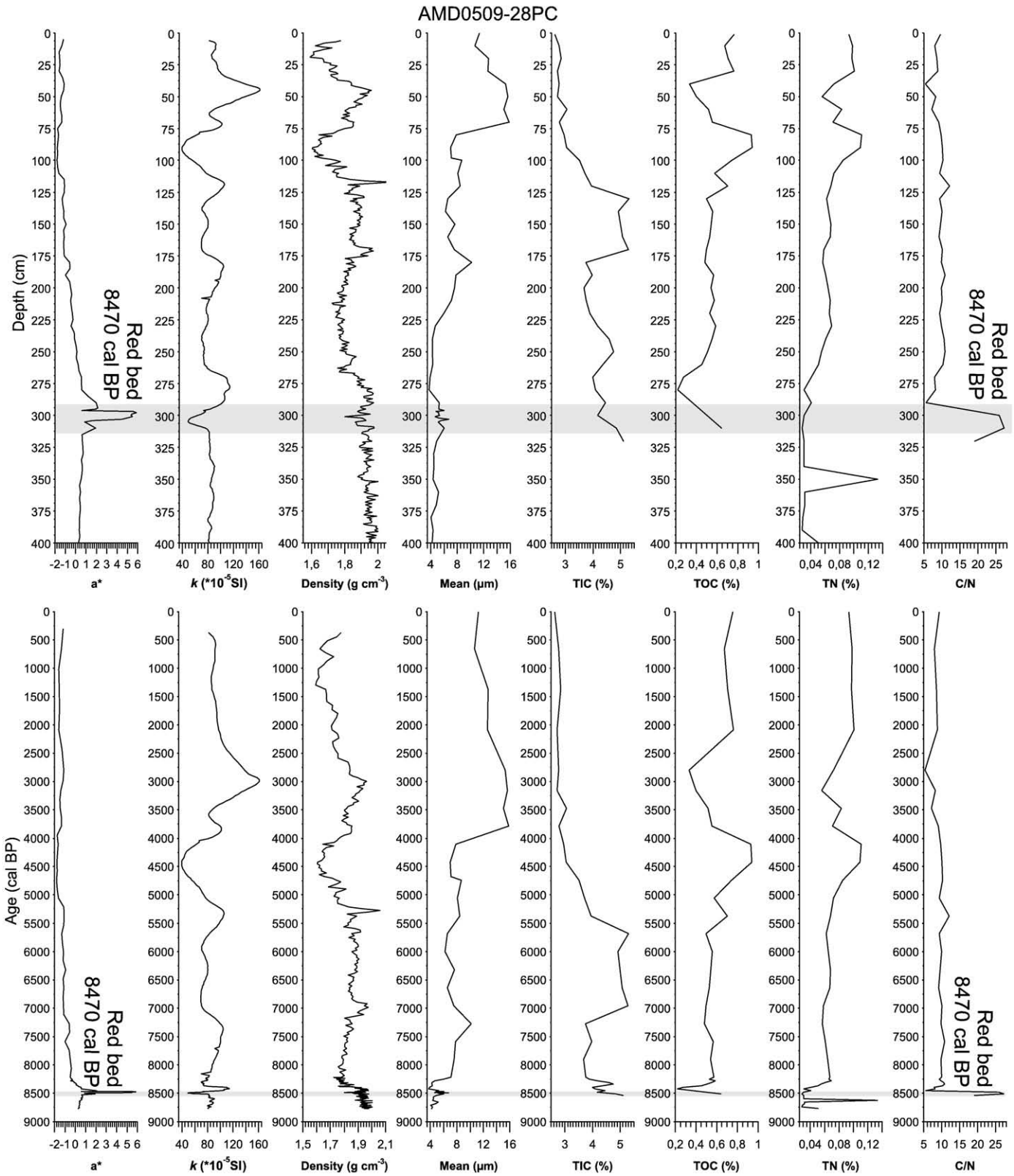

Fig. 7. Sedimentological, geochemical and physical properties of core 28 plotted on a depth scale (top), as well as on an age scale (bottom).

decrease to below zero above the red layer. Furthermore, the red bed is characterised by low *k* and TN values, almost no change in density, and high TIC, TOC and *C/N* ratios (Fig. 7). Below the red layer, all parameters show only minor variations except for one peak in TN at 350 cm. Above the red layer, *k*, density and mean grain sizes exhibit a similar pattern with a minimum at 100–75 cm and a subsequent maximum at 75–30 cm followed by a steady decrease of *k* and median grain sizes to the top. TOC and TN show an inverse pattern to these three parameters. TIC

has the greatest variability of all the cores recovered for this study. It is also characterised by a general opposite pattern to mean grain sizes. However, the decrease in TIC starts earlier (125 cm) than the increase of the mean of the grain size (75 cm, Fig. 7). *C/N* ratios oscillate around 9 (average: 9.25) above the red layer.

5. Interpretation and discussion

5.1. Core 27

The opposite pattern of a^* and *k* in the red bed confirms the assumption that the sediments of the red bed ascribed to the red rocks of the predominately Proterozoic Dubawnt Group are low in *k*. This means that if the red color increases, *k* decreases (Hall et al., 2001; Kerwin, 1996). The red sediments within the red bed are interpreted to have relatively high proportions of hematite (Kerwin, 1996) which has a two order of magnitude weaker *k* signal than ferrimagnetic components such as magnetite from other local outcrops (Hall et al., 2001). Further details about the red layer in this record can be found elsewhere (Lajeunesse and St-Onge, 2008; St-Onge and Lajeunesse, 2007). Above the red bed not only the red color is much lower but also *k* showing the same decreasing trend to the top of the core (Fig. 3). This difference was formerly explained by changes in grain size and density (St-Onge and Lajeunesse, 2007). Nevertheless, there is no sufficient explanation for the continuous decrease in density (and *k*). In order to test whether a change in grain sizes influences the decrease in *k* the fraction 10–100 μm was examined. This is one of the two fractions showing enhanced magnetic susceptibility with magnetite grain size (Dearing, 1994). The other fraction which is <0.01 μm was too small to be measured with the analyzer. Although, there is a decrease visible in the 10–100 μm fraction, this decrease is stepwise rather than continuous. In addition, as *X* also shows a decreasing trend, this decrease might be the result of dilution by organic matter and/or an increase in carbonates.

The continuous decrease of a^* above the red layer, although values are much smaller than in the red bed (Fig. 3), illustrates the decreasing importance of the Dubawnt Group as source for sediments in core 27 by remobilisation. Reduced remobilisation and hence less strong currents above the red layer and especially above 100 cm are also suggested by the small grain sizes (mean and low values of the 10–100 μm fraction, Fig. 3). The sediment distribution within Hudson Bay is extremely patchy. Postglacial sediments are only deposited in bathymetric lows and mainly consist of coarse material. Often there is no deposition in shallower areas. This was formerly attributed to currents which rework material from the shallower parts. This material is then redeposited in current protected lows or pockets where turbulence induced by marine currents is incapable of maintaining the particles in suspension (Henderson, 1990; Jennings et al., 2001). Therefore, we postulate that if currents get stronger, coarser material will be redistributed. As currents get weaker, only fine material is eroded and redeposited which is the case in core 27.

5.2. Core KUJ01

The 1890 ± 125 cal BP date at a core depth of only 47 cm (Fig. 4) appears to be older than expected. Although, the mean grain size is low, one would assume a high sedimentation rate at the proximity of a river mouth (19 km offshore Grande-Rivière-de-la-Baleine, 116 m water depth, c.f., Table 1). Isopach maps of the individual acoustic units at the mouth of Grande-Rivière-de-la-Baleine show that the sediment cover is generally thick (Gonthier et al., 1993) and rythmites were found in previous studies in that area before 8000 BP (Bilodeau et al., 1990). However, there is no change in lithology visible in core KUJ01, but the radiocarbon age of 1890 ± 125 cal BP at 47 cm suggests a rather low sedimentation rate. Therefore, we hypothesize that the dated shell fragment is reworked and/or comprises a larger reservoir effect than assumed. Indeed, a core recently recovered close to the sampling location of core KUJ01 reveals a recent sedimentation rate of 0.9 mm a^{-1} (Kuzyk et al., 2008), compared to hypothetical 0.25 mm a^{-1} for core KUJ01.

KUJ01 is also characterised by an increasing trend in TIC contents toward the top of the core. As there is an opposite pattern between TIC and productivity indicators such as TOC and TN, an autochthonous carbonate precipitation due to productivity seems to be unlikely. This suggests that an increasing amount of allochthonous carbonate originating from either reworked marine sediments or Paleozoic bedrock was brought to the coring location increasing the minerogenic proportion in the sediment. The increase in minerogenic matter is consistent with a rise in *k* and density through time. Additionally, the *C/N* ratio rises contemporaneously with the other parameters approaching values indicating a larger portion of allochthonous terrestrial organic matter to be incorporated in the sediments. Molar *C/N* ratios have been widely used to reconstruct the sources of organic matter in different depositional environments before (Haberzettl et al., 2007; Haberzettl et al., 2008; Meyers, 1994; Meyers, 1997; Meyers, 2003; Meyers and Lallier-Vergés, 1999; St-Onge and Hillaire-Marcel, 2001), including Hudson Bay (Lavoie et al., 2008). This method is based on the assumption that algal organic matter has molar *C/N* values commonly between 4 and 10, whereas higher plants produce organic matter with higher *C/N* ratios (Meyers, 1994). As organic matter in sediments often represents a mixture of terrestrial and aquatic material, it is assumed that the rising *C/N* ratios measured through time in KUJ01 also represent an increase in terrestrial input. Due to the contemporaneous rise of the parameters representing minerogenic input this might also be attributed to a more terrestrial source of that material. One factor might be an increased fluvial discharge of Grande-Rivière-de-la-Baleine. Alternatively, the river mouth approached the coring location as a result of the glacio-isostatic uplift in this area, exposing formerly water covered areas and bringing the (paleo-) shoreline closer to the coring location. Such a migration of the coastline remobilizing former marine sediments through fluvial incision has already been proposed in earlier works for the mouth of Grande-Rivière-de-la-Baleine (Gonthier et al., 1993) and Nastapoka River (Lajeunesse and Allard, 2003a). Similar processes were observed in many other depositional environments using *C/N* ratios as paleoshoreline proximity indicator (Haberzettl et al., 2005). As the ice receded toward the hinterland, emergence due to glacio-isostatic uplift raised former marine limits to elevations above present sea level (Gonthier et al., 1993). This would be in accordance with the increasing *C/N* and TIC values (Fig. 4). Carbonate containing marine sediments formerly covered by the protective water column and arenites with stromatolitic dolostone occurring immediately at the shore today (MNR, 2002) became exposed to erosion forming a potential source for the carbonate found in the sediment record of KUJ01. Nevertheless, a period of high discharge was also recorded at the mouth of Grande-Rivière-de-la-Baleine which produced over half of the uppermost stratigraphic layer and dispersed the suspension load seaward (Gonthier et al., 1993). Probably a combination of the two processes (increased discharge and glacio-isostatic uplift) is responsible for the increase in minerogenic matter and grain sizes as well as for the increased terrestrial contribution to the organic matter fraction recorded in the sediments of KUJ01.

Lignin studies on box cores suggest that the organic material found in southeastern Hudson Bay is mainly composed of a redistributed, fine, mineral-associated fraction of terrigenous carbon. This is supposed to derive mainly from resuspension of older coastal and inner shelf deposits, whereas most modern plant remains appear to be retained near river mouths due to hydrodynamic sorting (Kuzyk et al., 2008). The sorting results in preferential dispersal of fine sediments and retention of coarse sediments in coastal zones close to their river sources. Coarse materials (including organic matter) delivered by large southeastern Hudson Bay rivers appear to be trapped in localized

depressions near the coast (Kuzyk et al., 2008). Thus, although coastal material is constantly subjected to erosion and resuspension by waves, predominantly fine components undergo transport offshore (Kuzyk et al., 2008). These findings are supported by the results of core KUJ01 that show increased terrestrial organic input of very small grain size in the upper part of the core, implying that 19 km offshore is sufficient for effective sorting. As the organic fraction was not destroyed prior to grain size analysis, the grain size data point to the absence of larger organic compounds in the sediments.

5.3. Core 20 (Nastapoka Sound)

Constant small mean grain sizes (3 to 5.5 μm, Fig. 5) in core 20, retrieved from the Nastapoka Sound immediately north of the Lac-Guillaume-Delisle outlet, indicate that Lac-Guillaume-Delisle acted like a sediment trap only enabling the small sediment fraction to pass. Within Lac-Guillaume-Delisle itself, mean grain sizes vary from 15 to 4.6 μm (Lavoie et al., 2008). Leaving Lac-Guillaume-Delisle and entering Nastapoka Sound, the strong anticlockwise coastal currents of up to 15 to 20 cm s^{-1} in eastern Hudson Bay (Saucier et al., 2004) were then able to transport the sediment load to the coring location. According to the absence of grain size variation, contributions from the Nastapoka River, which is aside from Grande-Rivière-de-la-Baleine, one of the main rivers of eastern Hudson Bay (Henderson, 1990), appear to be of minor importance. Nastapoka River is located further to the north which means downstream of the currents as far as core 20 is concerned. If core 20 would be influenced by the Nastapoka River, variation in the grain sizes should be visible, as models for fluvial sedimentation in the Arctic marine environment indicate that inflowing sediment of all grain sizes is transported offshore during the summer (Henderson, 1990). Another conclusion to be drawn from the absence of marked grain size variation is that there seems to be a change in provenance at ~2400 cal BP. This change is highlighted by k, a^* and density (Fig. 5). The assumption appears to be justified as k was used as first-order indicator of sediment provenance in Hudson Strait in previous studies (Andrews et al., 1995; Hall et al., 2001). In these studies, changes in k were associated with changes in the contribution of sediments from various Precambrian outcrops surrounding and within the Strait, versus the diluting effect of detrital carbonate from Paleozoic sources underlying Hudson Strait. The increase or decrease in the mentioned proxies in core 20 from the Nastapoka Sound might be related to a change from reworked local sediments to sediments originating from the Canadian Shield, e.g., the Nastapoka Hills extending 4 to 7 km inland parallel to the curved Hudson Bay coast, in Archean granite–gneiss terrain (Lajeunesse and Allard, 2003a), yielding higher k values. Unfortunately, 2400 cal BP is only an approximation, as the age model beyond 1220 cal BP is only based on linear extrapolation. However, as there is no change in sedimentation visible in any of the parameters between 1220 and 2400 cal BP and because sedimentation rates above are relatively constant, a linear extrapolation of the age–depth model seems to be a reasonable approximation for this period. A change of the sediment source after 2400 cal BP also coincides with peaks of alluvial activity on the headland dividing the Nastapoka Sound from Lac-Guillaume-Delisle during the Late Holocene (i.e., from 2950 to 2750, 1900 to 1400, and 800 to 300 cal BP) (Lafortune et al., 2006). These are indicative for episodes of increased storminess allowing for fan formation in a cooler and more humid climate. Summed probability distributions of gelifluction and runoff starting ca. 2000 cal BP (Lafortune et al., 2006) confirm the wetter conditions. This increase in moisture also provides an increase in transport energy enabling a transport over larger distances which might be necessary to provide "inland" material for core 20 in the Nastapoka Sound causing the potential change in provenance indicated by our parameters. Single peaks or minima like the ones observed at ~3200 cal BP or 1050 cal BP are probably related to local event layers like tubidites and do not reflect large scale variations.

5.4. Core 17 (center of Hudson Bay marine system)

Core 17 located between Mansel and Nottingham Islands in the center of the Hudson Bay marine system (Fig. 1) has the highest temporal resolution of all recovered records. Although, the core is located in the anticipated spillway of the outburst flood of Lake Agassiz (Lajeunesse and St-Onge, 2008; St-Onge and Lajeunesse, 2007), its higher sedimentation rate did not allow the recovery of the red bed.

The slight increase in deposition after $415^{+85}/_{-115}$ cal BP (Fig. 2) seems to be contemporaneous to the rise in k (Fig. 6). k in turn mainly seems to be driven by changes in grain size which again shows a similar pattern to TIC, but an opposite pattern to TOC and TN (Fig. 6). The negative correlation of TIC and TN clearly demonstrates that the availability of the inorganic carbon is not related to biogenic production. Hence, it can be assumed that k and TIC reflect the availability of minerogenic matter in general. This means that the delivery of minerogenic matter increased with time, which also increased sedimentation rates in the upper part of the record.

Although, the absolute changes are very low, the distinct minimum in indicators of production (TOC, TN) between ~450 and 150 cal BP might be interpreted to be a response to the Little Ice Age being a result of lower production triggered by lower temperatures. In contrast, the rise of TOC and TN in the uppermost part of the core might be related to increasing 20th century temperatures. These might lead to an extended growth period which in turn might increase production and hence the availability of organic carbon. In another study from Hudson Strait performed close to core 28 from this study (Fig. 1), cold intervals during the seventeenth and nineteenth centuries are characterised by increased faunal abundances and decreased percentages of calcareous foraminifers (Jennings et al., 2001). These changes were interpreted to reflect greater mixing and cooling of bottom-water temperatures at these times, which supports the assumption of lower productivity due to cooler temperatures in core 17. Additionally, colder conditions might cause an extended ice cover which in turn might result in less production. According to that interpretation, the gradual decrease in productivity from the bottom of the record to 250 cal BP (Fig. 6) might be related to a continuing decrease in temperature. Similarly, July temperatures declined throughout the tundra regions of eastern Canada after 4000 BP (Kerwin et al., 2004).

The generally high TOC values observed in this core are also found in recent sediments of that area (Leslie, 1964; Pelletier, 1969). This might be explained by the setting of the coring location. Modeling results show that especially in fall, the center of the Hudson Bay marine system is influenced by strong currents deriving from all directions including Hudson Bay, Hudson Strait and Foxe Basin (Saucier et al., 2004). Although Hudson Bay can be regarded as oligotrophic during summer (Anderson and Roff, 1980) with a low rate of nutrient regeneration (Pett and Roff, 1982), the area north of Southampton–Coats–Mansel Islands receives exceptionally large increments of fine sediments including large amounts of fine organic particles from Foxe Basin ice (Anderson and Roff, 1980; Pelletier, 1969). This probably provides additional organic matter to the coring location of core 17. Sedimentation is also sufficiently rapid in this area to inhibit long-continued oxidation of the particles containing organic carbon, and thus organic carbon contents remain high (Pelletier, 1969).

Prevailing currents from all directions also impede a more precise provenance analysis. However, low absolute k and high TIC values point to reworked marine sediments or Paleozoic limestone underlying a large part of Hudson Bay and Hudson Strait (Andrews and MacLean, 2003; Henderson, 1990) as a main source. Paleozoic limestones also occur on Coats, Mansel and Southampton Islands in northern Hudson Bay, and in Foxe Basin as well as on western Baffin Island (Andrews and MacLean, 2003). In a core approximately 100 km

to the west of core 17, reworked palynomorphs of Paleozoic age are common to abundant in Quaternary sediments. These palynomorphs probably originate from Paleozoic rocks in Hudson Bay. The abundance indicates intense erosion and subsequent transport (Bilodeau et al., 1990). This is in accordance with the observation that percentages of carbonates in surficial sediments are generally high in northern Hudson Bay indicating little sediment input from the Precambrian terrain (Henderson, 1990). Paleozoic limestones from the floor of Hudson Bay and Hudson Strait deposited during Heinrich Events in the North Atlantic were also used as most diagnostic tracers linking source and depositional areas (Andrews and MacLean, 2003; Andrews and Tedesco, 1992; Bond et al., 1992), demonstrating the abundance of that material in Hudson Bay and Hudson Strait.

Boxplots of whole core magnetic susceptibility distinguishing between the major basins of Hudson Strait and Hudson Bay show least variability and lowest absolute values in northern Hudson Bay and the Western Basin of Hudson Strait (Andrews et al., 1995). This is west and east of the coring location of core 17 and confirms the low absolute values of *k* and high TIC values found in this record. These data are also in accordance with previous observations made east and west of the coring location of core 17: marine sedimentation in Hudson Strait was not greatly influenced by processes directing sediments into the strait from its flanks, i.e., Precambrian sources bordering the Paleozoic rocks to the north and south and at the islands at the western end of Hudson Strait (Andrews et al., 1995). This is confirmed by the *C*/*N* ratios measured in core 17 which indicate a predominantly marine source of the organic material. If more terrestrial material from the flanks is brought to the coring location, an increase of the *C*/*N* ratios would be assumed.

5.5. Core 28 (Western Basin of Hudson Strait)

In the area around core 28, many other records mainly focusing on surface samples or the global Late Quaternary history have been studied before (MacLean, 2001). The age–depth model of core 28 seems to be typical for Hudson Strait during the covered time span. Other cores taken nearby yield the same high sedimentation rate before, during and shortly after the deposition of the red layer, as well as much lower sedimentation rates in the upper parts of the records (Andrews et al., 1995; Kerwin, 1996). However, as assumed (Andrews et al., 1995) and demonstrated before (St-Onge and Lajeunesse, 2007), the uppermost part of these cores is missing, resulting in a unique opportunity to study the complete sequence of postglacial paleoenvironmental variations in core 28. Most variations in the parameters of core 28 primarily seem to be related to sediment provenance. The most striking feature, the peak in red color (red bed), was already attributed to the sediments deposited during the last outburst flood of Lake Agassiz probably originating from the remobilisation of red sediments originating from the Dubawnt Group (Lajeunesse and St-Onge, 2008; St-Onge and Lajeunesse, 2007). Detailed descriptions and interpretations of the red layer in this record can be found in the above papers. As in core 17, after that event, sediments from that source seem to be unimportant. The absence of variations in all parameters below the red layer (Fig. 7) might be explained by the high sedimentation rate and the resulting short-covered time span before the outburst flood (Fig. 2). This is probably also the reason for the absence of rythmites reported below unstratified greenish silty clay from other records before the outburst flood (Bilodeau et al., 1990). From 8470 cal BP to ~4500 cal BP, carbonate-rich sediments of rather low magnetic susceptibility dominate, probably originating from Paleozoic limestone sources underlying Hudson Strait. A productively driven carbonate precipitation is rather unlikely, as during that period TOC and TN stay rather low and increase only after that period. From 4000 cal BP onwards, coarser material with higher magnetic susceptibility is transported to the coring location. A similar relationship between texture and composition has been outlined before showing that igneous and metamorphic rocks produce a coarser matrix than carbonates (Henderson, 1990). The coarser material of higher magnetic susceptibility potentially originates from Precambrian (granitoids) sources (e.g., mainland southern shore) and dilutes the carbonatic deposits. Unlike in core 17 where almost no material bearing high magnetic susceptibility was present, in core 28 as well as in the western portion of Hudson Strait, an important control on magnetic susceptibility seems to be the detrital carbonate eroded from the Paleozoic bedrock within Hudson Strait, Hudson Bay and the Foxe Basin. As calcite is a diamagnetic mineral increased detrital carbonate deposition will yield lowered magnetic susceptibility values (Hall et al., 2001) and vice versa.

The low organic contents especially before 5500 cal BP are also mirrored by high absolute density values (>1.9 g cm^{-3}). At the same time, low biogenic production related to cold Arctic water masses and dense seasonal sea-ice cover prevailed until at least 6000 BP (~6800 cal BP), and probably 4000 BP (~4500 cal BP) in a core located approximately 350 km further to the west (Bilodeau et al., 1990). Furthermore, TOC and TN maxima in core 28 at around 5000 to 4000 cal BP (Fig. 7) are contemporaneous to low lake levels at Lac des Pluviers (Fig. 1) attributed to warm conditions from 5400 to 3500 BP (~6300–3700 cal BP) showing the most important lowering between 4600 and 4100 BP (~5400–4500 cal BP) (Payette and Filion, 1993). Increased summertime insolation and the final disappearance of the Laurentide Ice Sheet probably also caused July temperatures throughout eastern Canada to peak between approximately 5000 and 3500 BP (~5800–3700 cal BP) (Kerwin et al., 2004), which is also concordant to the TOC and TN maxima in core 28 (Fig. 7). Another low lake level was reported from Lake Kachishayoot before 3200 BP (~3400 cal BP) (Miousse et al., 2003) and a limited alluvial fan activity was observed in the Lac-Guillaume-Delisle area (see Fig. 1 for location) prior to 3500 cal BP corresponding to a relatively mild and dry regime (Lafortune et al., 2006). These terminal ages of 3500 and 3200 cal BP, respectively are contemporaneous to the end of the increased TOC and TN values in core 28 starting after 5500 cal BP (Fig. 7). Additionally, the minima in TOC and TN after 4000 cal BP are contemporaneous to a marked cooling inferred from palynostratigraphic analysis of peat sections near the tree line on the eastern coast of Hudson Bay starting by 3200 BP (~3400 cal BP)(Allard and Seguin, 1987). This coherence between temperature reconstructed on the terrestrial realm and organic matter indicators in marine core 28 suggests a sensitivity of those parameters to temperature as well as a similar development in the sea and on land as *C*/*N* ratios in core 28 indicate that terrestrial organic input is of minor importance during postglacial times. However, due to the coarse temporal resolution in the upper part of core 28, no response to the Little Ice Age is visible.

6. Conclusions

This study has shown that sediments of the Hudson Bay complex are perfectly suited to reconstruct environmental changes during postglacial conditions, provided that the “right spot” with a high sedimentation rate is chosen and the top of the cores is preserved, which was not always the case in previous studies. High-resolution measurements of physical and geochemical properties reveal changes in the transport of minerogenic material. Although, waters from Hudson Bay show an anticlockwise circulation pattern, nothing of that pattern was found in the sedimentological record. Due to their location each of the five sedimentary archives investigated in this study reacted sensitive to different environmental influences, i.e., transport from different provenances reflected by different indicators or climate. However, a link between the different archives might be seen in a decrease in minerogenic supplies which was observed in central Hudson Bay, whereas the opposite trend was found in Hudson Strait and off the mouth of Grande-Rivière-de-la-Baleine since the last outburst flood of Lake Agassiz–Ojibway.

Many records yield a provenance signal allowing to distinguish between Dubawnt Group sediments (a^*, k), Paleozoic limestone sources underlying parts of Hudson Bay and Strait (TIC, k) and Precambrian granitoids from the Canadian Shield (TIC, k). In this context, the previously assumed relationship between intense red color and low magnetic susceptibility due to hematite in sediments originating from the Dubawnt Group was confirmed. Above the red bed associated with the final outburst flood of Lake Agassiz–Ojibway, the importance of the Dubawnt Group as a sediment source decreases or vanishes completely.

Often it is difficult to figure out the mode of transport responsible for the changes seen in the archives. Except for core 20 from Nastapoka Sound where according to the grain size measurements it is probably negligible, it is hard or impossible to assess the role of sediment rafting in and on sea-ice. Some records yield sporadic dropstones but no clear pattern is evident as the sediments are generally composed of fine material.

On the cores where organic matter indicators were measured, trends were associated with changes in productivity linked to climatic changes and are similar to those inferred from terrestrial archives. Productivity indicators in this study suggest colder conditions in Hudson Strait until ~4500 cal BP followed by warmer conditions until ~4000 cal BP. Thereafter, a cool interval lasting until approximately ~2000 cal BP followed. A gradual decrease in temperature was then observed in the other core from Hudson Strait reaching its lowest values during the Little Ice Age period before it rises again.

Acknowledgements

We would like to thank Antoon Kuijpers and an anonymous reviewer for suggestions on the original version of the manuscript. T.H. was supported by a postdoctoral fellowship scholarship provided by FQRNT (Fonds québécois de la recherche sur la nature et les technologies). This study was also supported by a FQRNT new researcher grant to G.S., by NSERC (Natural Sciences and Engineering Research Council of Canada) discovery grants to G.S. and P.L. and by ArcticNet (Network of Centers of Excellence of Canada) grants and ship-time to P.L. Finally, the authors also acknowledge the help of M. Lajoie and V. Gagnon in the laboratory as well as the help of M. Paiement during coring. This constitutes GEOTOP contribution no. 2009-0021.

References

Allard, M., Seguin, M.K., 1985. La déglaciation d´une partie du versant hudsonien québécois: bassins des Rivières Nastapoca. Sheldrake et à la L`eau Claire. Géographie physique et Quaternaire 39, 13–24.

Allard, M., Seguin, M.K., 1987. The Holocene evolution of permafrost near the tree line, on the eastern coast of Hudson Bay (northern Quebec). Canadian Journal of Earth Sciences 24, 2206–2222.

Allard, M., Tremblay, G., 1983. Les processus d'érosion littorale périglaciaire de la région de Poste-de-la-Baleine et des Iles Manitounuk sur la côte est de la mer d'Hudson, Canada. Zeitschrift für Geomorphologie, Supplement Band 47, 27–60.

Alley, R.B., Ágústsdóttir, A.M., 2005. The 8 k event: cause and consequences of a major Holocene abrupt climate change. Quaternary Science Reviews 24, 1123–1149.

Anderson, J.T., Roff, J.C., 1980. Seston ecology of the surface waters of Hudson Bay. Canadian Journal of Fisheries and Aquatic Sciences 37, 2242–2253.

Andrews, J.T., MacLean, B., 2003. Hudson Strait ice streams: a review of stratigraphy, chronology and links with North Atlantic Heinrich events. Boreas 32, 4–17.

Andrews, J.T., MacLean, B., Kerwin, M., Manley, W., Jennings, A.E., Hall, F., 1995. Final stages in the collapse of the Laurentide Ice Sheet, Hudson Strait, Canada, NWT: ^{14}C AMS dates, seismic stratigraphy, and magnetic susceptibility logs. Quaternary Science Reviews 14, 983–1004.

Andrews, J.T., Tedesco, K., 1992. Detrital carbonate-rich sediments, northwestern Labrador Sea: implications for ice-sheet dynamics and iceberg rafting (Heinrich) events in the North Atlantic. Geology 20, 1087–1090.

Barber, D.C., Dyke, A., Hillaire-Marcel, C., Jennings, A.E., Andrews, J.T., Kerwin, M.W., Bilodeau, G., McNeely, R., Southon, J., Morehead, M.D., Gagnon, J.M., 1999. Forcing of the cold event of 8,200 years ago by catastrophic drainage of Laurentide lakes. Nature 400, 344–348.

Bégin, Y., Bérubé, D., Grégoire, M., 1993. Downward migration of coastal conifers as a response to recent land emergence in eastern Hudson Bay, Québec. Quaternary Research 40, 81–88.

Bilodeau, G., Vernal, A.d., Hillaire-Marcel, C., Josenhans, H., 1990. Postglacial paleoceanography of Hudson Bay: stratigraphic, microfaunal, and palynological evidence. Canadian Journal of Earth Sciences 27, 946–963.

Bond, G., Heinrich, H., Broecker, W., Labeyrie, L., McManus, J., Andrews, J., Huon, S., Jantschik, R., Clasen, S., Simet, C., Tedesco, K., Klas, M., Bonani, G., Ivy, S., 1992. Evidence for massive discharges of icebergs into the North Atlantic ocean during the last glacial period. Nature 360, 245–249.

Dearing, J., 1994. Environmental Magnetic Susceptibility. Using the Bartington MS2 System. Chi Publishing, Kentworth. 104 pp.

Dyke, A.S., Prest, V.K., 1987. Late Wisconsinan and Holocene History of the Laurentide Ice Sheet. Géographie physique et Quaternaire 2, 237–263.

Gonthier, N., d'Anglejan, B., Josenhans, H.W., 1993. Seismo-stratigraphy and sedimentology of Holocene sediments off Grande Rivière de la Baleine, southeastern Hudson Bay, Québec. Géographie physique et Quaternaire 47, 147–166.

Haberzettl, T., Corbella, H., Fey, M., Janssen, S., Lücke, A., Mayr, C., Ohlendorf, C., Schäbitz, F., Schleser, G.H., Wille, M., Wulf, S., Zolitschka, B., 2007. Lateglacial and Holocene wet–dry cycles in southern Patagonia: chronology, sedimentology and geochemistry of a lacustrine record from Laguna Potrok Aike, Argentina. The Holocene 17, 297–310.

Haberzettl, T., Fey, M., Lücke, A., Maidana, N., Mayr, C., Ohlendorf, C., Schäbitz, F., Schleser, G.H., Wille, M., Zolitschka, B., 2005. Climatically induced lake level changes during the last two millennia as reflected in sediments of Laguna Potrok Aike, southern Patagonia (Santa Cruz, Argentina). Journal of Paleolimnology 33, 283–302.

Haberzettl, T., Kück, B., Wulf, S., Anselmetti, F., Ariztegui, D., Corbella, H., Fey, M., Janssen, S., Lücke, A., Mayr, C., Ohlendorf, C., Schäbitz, F., Schleser, G.H., Wille, M., Zolitschka, B., 2008. Hydrological variability in southeastern Patagonia and explosive volcanic activity in the southern Andean Cordillera during oxygen isotope stage 3 and the Holocene inferred from lake sediments of Laguna Potrok Aike, Argentina. Palaeogeography, Palaeoclimatology, Palaeoecology 259, 213–229.

Hall, F.R., Andrews, J.T., Kerwin, M., Smith, L.M., 2001. Studies of sediment colour, whole-core magnetic susceptibility, and sediment magnetism of the Hudson Strait–Labrador Shelf region: *CSS Hudson* cruise 90023 and 93034. In: MacLean, B. (Ed.), Marine Geology of Hudson Strait and Ungava Bay, Eastern Arctic Canada: Late Quaternary Sediments, Depositional Environments, and Late Glacial–Deglacial History Derived from Marine and Terrestrial Studies: Geological Survey of Canada Bulletin, 566, pp. 161–170.

Hardy, I., 2001. Composition of sediments in Hudson Strait and Ungava Bay. In: MacLean, B. (Ed.), Marine Geology of Hudson Strait and Ungava Bay, Eastern Arctic Canada: Late Quaternary Sediments, Depositional Environments, and Late Glacial–Deglacial History Derived from Marine and Terrestrial Studies: Geological Survey of Canada Bulletin, 566, pp. 147–159.

Hare, A., Stern, G.A., Macdonald, R.W., Kuzyk, Z.Z., Wang, F., 2008. Contemporary and preindustrial mass budgets of mercury in the Hudson Bay Marine System: the role of sediment recycling. Science of the Total Environment 406, 190–204.

Henderson, P.J., 1990. Provenance and Depositional Facies of Surficial Sediments in Hudson Bay, a Glaciated Epeiric Sea. University of Ottawa, Ottawa. 287 pp.

Hill, P.R., Simard, A., Héquette, A., 1999. High-resolution seismic stratigraphy of late Quaternary deposits in Manitounouk Sound, northern Quebec: effects of rapid postglacial emergence. Canadian Journal of Earth Sciences 36, 549–563.

Hillaire-Marcel, C., 1976. La déglaciation et le relèvement isostatique sur la côte est de la baie d'Hudson. Cahiers de Géographie de Québec 20, 185–220.

Hughen, K., Baillie, M., Bard, E., Bayliss, A., Beck, J., Blackwell, P., Buck, C., Burr, G., Cutler, K., Damon, P., Edwards, R., Fairbanks, R., Friedrich, M., Guilderson, T., Herring, C., Kromer, B., McCormac, F., Manning, S., Ramsey, C., Reimer, P., Reimer, R., Remmele, S., Southon, J., Stuiver, M., Talamo, S., Taylor, F., van der Plicht, J., Weyhenmeyer, C., 2004. Marine04 Marine radiocarbon age calibration, 0–26 cal kyr BP. Radiocarbon 46, 1059–1086.

Jenner, K.A., Piper, D.J.W., 2002. Grande Rivière de la Baleine, Hudson Bay, Quebec — 1000 years of sedimentation. Geological Survey of Canada. 2002-E10.

Jennings, A.E., Vilks, G., Deonarine, B., Silis, A., Weiner, N., 2001. Foraminiferal biostratigraphy and paleoceanography. In: MacLean, B. (Ed.), Marine Geology of Hudson Strait and Ungava Bay, Eastern Arctic Canada: Late Quaternary Sediments, Depositional Environments, and Late Glacial–Deglacial History Derived from Marine and Terrestrial Studies: Geological Survey of Canada Bulletin, 566, pp. 127–146.

Josenhans, H., Zevenhuizen, J., 1990. Dynamics of the Laurentide Ice Sheet in Hudson Bay, Canada. Marine Geology 92, 1–26.

Josenhans, H., Balzer, S., Henderson, P., Nielson, E., Thorliefson, H., Zevenhuizen, J., 1988. Preliminary seismostratigraphic and geomorphic interpretations of the Quaternary sediments of Hudson Bay. Current Research, Part B, Geological Survey of Canada, Paper 88-1B, 271–286.

Kerwin, M.W., 1996. A regional stratigraphic isochron (ca. 8000 ^{14}C yr B.P.) from final deglaciation of Hudson Strait. Quaternary Research 46, 89–98.

Kerwin, M.W., Overpeck, J.T., Webb, R.S., Anderson, K.H., 2004. Pollen-based summer temperature reconstructions for the eastern Canadian boreal forest, subarctic, and Arctic. Quaternary Science Reviews 23, 1901–1924.

Kuzyk, Z.Z.A., Goñi, M.A., Stern, G.A., Macdonald, R.W., 2008. Sources, pathways and sinks of particulate organic matter in Hudson Bay: evidence from lignin distributions. Marine Chemistry 112, 215–229.

Lafortune, V., Filion, L., Hétu, B., 2006. Impacts of Holocene climatic variations on alluvial fan activity below snowpatches in subarctic Québec. Geomorphology 76, 375–391.

Lajeunesse, P., 2008. Early Holocene deglaciation of the eastern coast of Hudson Bay. Geomorphology 99, 341–352.

Lajeunesse, P., Allard, M., 2003a. Late Quaternary deglaciation, glaciomarine sedimentation and glacioisostatic recovery in the Rivière Nastapoka Area, Eastern Hudson Bay, Northern Québec. Géographie physique et Quaternaire 57, 65–83.
Lajeunesse, P., Allard, M., 2003b. The Nastapoka drift belt, eastern Hudson Bay: implications of a stillstand of the Quebec–Labrador ice margin in the Tyrrell Sea at 8 ka BP. Canadian Journal of Earth Sciences 40, 65–76.
Lajeunesse, P., St-Onge, G., 2008. The subglacial origin of the Lake Agassiz–Ojibway final outburst flood. Nature Geoscience 1, 184–188.
Lavoie, C., Hill, P.R., Allard, M., St-Onge, G., Lajeunesse, P., 2008. High-resolution seismostratigraphy and sedimentological properties of late- and postglacial sediments in Lac Guillaume-Delisle Estuary and Nastapoka Sound, eastern Hudson Bay. Canadian Journal of Earth Sciences 45, 427–441.
Laymon, C.A., 1992. Glacial geology of western Hudson Strait, Canada, with reference to Laurentide Ice Sheet dynamics. Geological Society of America Bulletin 104, 1169–1177.
Leslie, R.J., 1964. Sedimentology of Hudson Bay. District of Keewatin: Geological Survey of Canada Paper, pp. 48–63.
MacLean, B., 2001. Introduction: geographic setting and studies. In: MacLean, B. (Ed.), Geological Survey of Canada, Bulletin, 566, pp. 5–17.
McNeely, R., Dyke, A.S., Southon, J.R., 2006. Canadian marine reservoir ages, preliminary data assessment. Geological Survey of Canada, Open File 5049, 3.
Meyers, P.A., 1994. Preservation of elemental and isotopic source identification of sedimentary organic matter. Chemical Geology 114, 289–302.
Meyers, P.A., 1997. Organic geochemical proxies of paleoceanographic, paleolimnologic, and paleoclimatic processes. Organic Geochemistry 27, 213–250.
Meyers, P.A., 2003. Applications of organic geochemistry to paleolimnological reconstructions: a summary of examples from the Laurentian Great Lakes. Organic Geochemistry 34, 261–289.
Meyers, P.A., Lallier-Vergés, E., 1999. Lacustrine sedimentary organic matter records of Late Quaternary paleoclimates. Journal of Paleolimnology 21, 345–372.
Miousse, L., Bhiry, N., Lavoie, M., 2003. Isolation and water-level fluctuations of Lake Kachishayoot, Northern Québec, Canada. Quaternary Research 60, 149–161.
MNR, 2002. Geological Map of Québec. Ministère des Ressources Naturelles.
Overpeck, J., Hughen, K., Hardy, D., Bradley, R., Case, R., Douglas, M., Finney, B., Gajewski, K., Jacoby, G., Jennings, A., Lamoureux, S., Lasca, A., MacDonald, G., Moore, J., Retelle, M., Smith, S., Wolfe, A., Zielinski, G., 1997. Arctic environmental change of the last four centuries. Science 278, 1251–1256.
Payette, S., Filion, L., 1993. Holocene water-level fluctuations of a subarctic lake at the tree line in northern Quebec. Boreas 22, 7–14.
Pelletier, B.R., 1969. Submarine physiography, bottom sediments, and models of sediment transport in Hudson Bay. In: Hood, P.J. (Ed.), Earth Science Symposium on Hudson Bay. Geological Survey of Canada, Dept. of Energy, Mines and Resources, Ottawa, pp. 100–135.
Pett, R.J., Roff, J.C., 1982. Some observations and deductions concerning the deep waters of Hudson Bay. Le Naturaliste Canadien (Rev. Écol. Syst.), 109, pp. 767–774.
Prinsenberg, S.J., 1986. The circulation pattern and current structure of Hudson Bay. In: Martini, I.P. (Ed.), Canadian Inland Seas. Elsevier, Elsevier Oceanography Series, pp. 187–204.
Saucier, F.J., Senneville, S., Prinsenberg, S., Roy, F., Smith, G., Gachon, P., Caya, D., Laprise, R., 2004. Modelling the sea ice-ocean seasonal cycle in Hudson Bay, Foxe Basin and Hudson Strait, Canada. Climate Dynamics 23, 303–326.
Sawada, M., Gajewski, K., de Vernal, A., Richard, P., 1999. Comparison of marine and terrestrial Holocene climatic reconstructions from northeastern North America. The Holocene 9, 267–277.
Shilts, W.W., 1986. Glaciation of the Hudson Bay region. In: Martini, I.P. (Ed.), Canadian Inland Seas. Elsevier, Elsevier Oceanography Series, pp. 55–78.
St-Onge, G., Hillaire-Marcel, C., 2001. Isotopic constraints of sedimentary inputs and organic carbon burial rates in the Saguenay Fjord, Quebec. Marine Geology 176, 1–22.
St-Onge, G., Lajeunesse, P., 2007. Flood-induced turbidites from northern Hudson Bay and western Hudson Strait: a two-pulse record of Lake Agassiz final outburst flood? In: Lykousis, V., Sakellariou, D., Locat, J. (Eds.), Submarine Mass Movements and Their Consequences Springer, Advances in Natural and Technological Hazards Research, vol. 27, pp. 129–137.
Stuiver, M., Reimer, P., Reimer, R., 2005. Calib 5.0. [WWW program and documentation].
von Grafenstein, U., Erlenkeuser, H., Müller, J., Jouzel, J., Johnsen, S., 1998. The cold event 8200 years ago documented in oxygen isotope records of precipitation in Europe and Greenland. Climate Dynamics 14, 78–81. doi:10.1007/s003820050210.
Weinelt, M., 1996–2004. Online Map Creation.